Linear Chain Antiferromagnetism in Copper Benzoate

Muneyuki DATE, Hitoshi YAMAZAKI,[*] Mitsuhiro MOTOKAWA
and Shuichi TAZAWA[**]

*Department of Physics, Faculty of Science, Osaka University
Toyonaka, Osaka*

Various magnetic properties of one dimensional antiferromagnet $Cu(C_6H_5COO)_2$ $\cdot 3H_2O$ were investigated by means of magnetic susceptibility, magnetic torque, NMR, and ESR measurements. The results show that this compound is one of the best one dimensional antiferromagnets known at present. An intrachain exchange interaction J/K was estimated to be $-8.6\pm1°K$ while no second order phase change was found down to $1.4°K$. ESR line width at room temperature was not explained by an usual treatment and an anisotropic exchange effect was newly taken into account. However, other anomalies of the line width such as the frequency, temperature, and angular dependences appeared at low temperature regions were not yet explained.

§1. Introduction

Recently, magnetism of low dimensional spin systems such as one or two dimensional ferro- or antiferromagnets has been investigated with growing interests and a number of substances have been studied by many researchers. One of the most attractive problems to be expected in these substances may be a physical property associating with an anomalously large effect of the short range order. In usual three dimensional magnets, the short range order effect appears near the critical temperature T_c or T_N but in one or two dimensional magnets it is not necessarily so. This is because of the fact that the transition temperature goes down to very low temperature compared with a value of zJ/k, where J means the main exchange interaction in a chain or plane and z is the number of nearest neighbor spins. So it gives rise to a fact that in a wide temperature region between T_c or T_N and zJ/k, spins in a chain or plane are inclined to align to each other but the alignment is confined so as to exclude the long range order. Accordingly, such an alignment should be of the short range order. One can then study various properties of spin-spin correlations by investigating well developed short range order spin systems in these substances.

Now, we confine ourselves to the problem of one dimensional antiferromagnets consisting of Heisenberg like spins. An exact mathematical solution of a Heisenberg linear chain has not yet been obtained but the fact that there

---

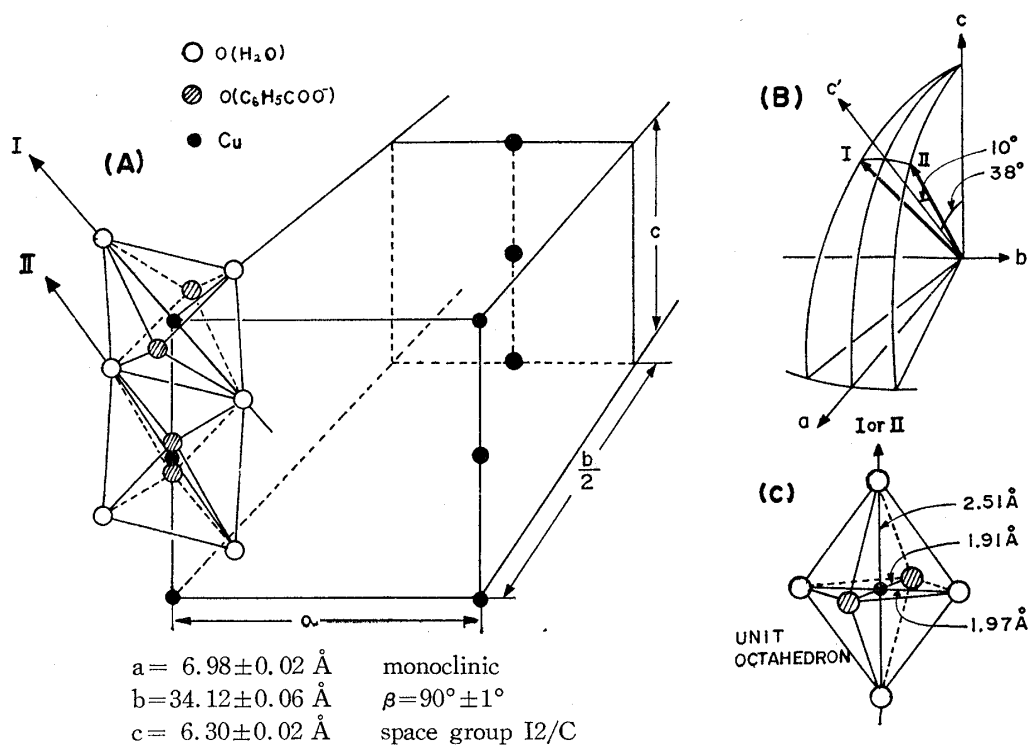[*] Present address: Institute of Solid State Physics, University of Tokyo, Roppongi, Tokyo.
[**] Present address: Research Division, Shinko Electric Works, Isé, Mie Prefecture.

is no second order phase transition in this system, is well known. Bonner and Fisher[1] obtained exact solutions of finite Heisenberg spin rings up to eleven spins and they extrapolated their results to an infinite spin chain. On the other hand, a typical example of the one dimensional antiferromagnetism was found in $KCuF_3$ by Hirakawa and his collaborators.[2] The NMR study by them,[3] the neutron diffraction experiment done by the Brookhaven group,[4] and the ESR study performed by Ikebe and one of the present authors (M. D.)[5] revealed that this compound is undoubtedly one of the best linear chain antiferromagnets known at present.

About a few years before these studies, we found that an organic copper compound, copper benzoate trihydrate $Cu(C_6H_5COO)_2 3H_2O$, can be considered as a good example of linear chain antiferromagnet and a preliminary report was published in 1963.[6] As will be seen in the next section, the linear chain spin structure is strikingly well established in this compound. Because of some complexity of the anisotropy axis in this crystal, the detailed analysis has not been performed till today. Recently, we completed the experiments of the magnetic susceptibility, magnetic torque, proton magnetic resonance and electron spin resonance and could analyze the main part of these results. In the next section a brief survey of the crystal structure will be presented and preparation of the specimen is shown in §3. The experimental results and the analysis on the magnetic susceptibility, NMR and ESR studies will be discussed in §§4 ~6, respectively and an anisotropic exchange interaction in an antiferromagnetic linear chain will be considered in the last section in connection with the ESR line width.

§2. Crystal structure

The crystal structure of copper benzoate trihydrate was determined by Koizumi et al.[7] This compound crystalizes in a monoclinic system, space group $I2/c$, with four chemical formula units in a unit cell of dimensions, $a=6.98$, $b=34.12$, $c=6.30 \text{Å}$ with $\beta \fallingdotseq 90°$. There are two kinds of benzoate groups and the carboxyl oxygen atoms of benzoate group I are in direct contacts with copper atoms, while those of group II are coordinated to copper atoms through water molecules. Each copper atom is situated at the center of a deformed octahedron consisted of four water molecules and two oxygen atoms from benzoate group I. The octahedra are linked, by sharing two water molecules, into a column parallel to the c-axis. A schematic view of the crystal structure is shown in Fig. 1(A) where benzoate groups are not drawn for simplicity. As is easily seen from the figure, a fairly strong superexchange interaction can be expected between copper spins along the c-axis whereas exchange interactions between spins in a c-plane may be so small that one can regard the spin system as a bundle of magnetic linear chains along the c-axis. There may be a very weak exchange coupling between chains along the a-axis

O O(H₂O)

⊘ O(C₆H₅COO⁻)

● Cu

(A)

(B)

(C)

a = 6.98±0.02 Å   monoclinic
b = 34.12±0.06 Å   β = 90°±1°
c = 6.30±0.02 Å   space group I2/C

Fig. 1. Crystal structure Cu(C₆H₅COO)₂3H₂O.

via a path Cu−H₂O−H₂O−H₂O−Cu but this may be negligible compared with the coupling in a chain. The central water molecule in this path is not drawn in Fig. 1(A). If one considers the magnetism below 1°K, the two dimensional spin coupling via this path should be taken into account. However, the three dimensional spin ordering in this compound cannot be expected even when the temperature decreases somewhat below 1°K because of the following reason: The distance between two copper atoms situated at 0, 0, 0 and 1/2, 1/2, 0 positions is very far and is 17.4 Å so that the exchange interaction may be extremely weak. Accordingly, one cannot estimate the three dimensional critical temperature of this crystal at least at present.

As is mentioned before, each copper atom is surrounded by six ligands forming a distorted octahedron. Among the six interatomic distances between copper and its ligand atoms, four have short distances (1.91 and 1.97 Å) and two have a long distance (2.51 Å). This means that the local symmetry of Cu²⁺ spin is nearly tetragonal and the directions of two inequivalent tetragonal axes I and II are shown in Fig. 1(B). The ground state wave function of Cu²⁺ ion may mainly consist of $x^2 - y^2$ type function, as is usually seen in hydrated copper salt. A sketch of an octahedron is shown in Fig. 1(C). The resultant paramagnetic principal axes of this compound are a', b and c'-axes where c'-axis is defined as in Fig. 1(B) and a'-axis is taken so as to perpendicular to b and c'-axes, because of the strong exchange interaction in a linear chain. This fact was verified by doing the magnetic susceptibility and para-

magnetic resonance measurements as will be shown later. It is necessary to show the positions of protons for analyzing NMR spectra. These informations will be given in addition to proton resonance data.

§3. Preparation of the specimen

Since this compound has very small solubility in water, the diffusion method was applied to prepare single crystals of measurable size. As is illustrated in Fig. 2, $CuSO_4 5H_2O$ and C_6H_5COONa crystals are put in two beakers A and B separately and then water is introduced into both beakers very quietly till the water level is far up beyond the edge of beaker A. By the chemical reaction between slowly diffused Cu^{2+} and $C_6H_5COO^-$ ions, thin needle like single crystals are obtained after one or two weeks as are schematically shown in Fig. 2. The single crystal is light blue and shows perfect cleavage parallel to a well developed *ac*-plane. Care should be taken to remove twined crystals.
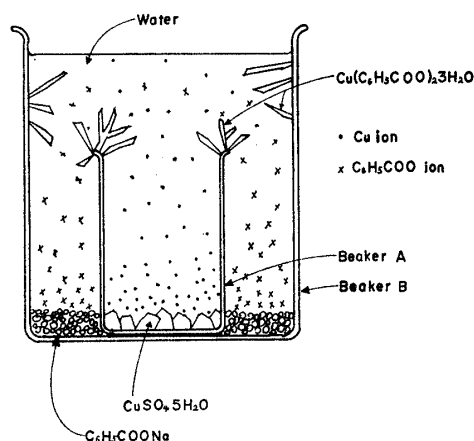

Fig. 2. Schematic view of making single crystals of copper benzoate. Crystals were grown at room temperature.

§4. Magnetic susceptibilities and intrachain exchange interaction

The static susceptibility and magnetic torque were measured by using an automatically controlled Faraday type magnetometer and twin-phototube balanced torque meter, respectively. Powdered susceptibility was measured to estimate the Curie-Weiss constant θ and the result is shown by a $1/\chi_g - T$ curve in Fig. 3, where χ_g represents the gram susceptibility in e.m.u. θ was determined to be $\theta = -9 \pm 4°K$. Accordingly, the superexchange interaction along a linear chain is antiferromagnetic. The $1/\chi_g$ curve shows a deviation from the Curie-Weiss law below near 40°K. So, a detailed susceptibility measurement on single crystal below 50°K was done as is summalized in Fig. 4. A broad maximum of the susceptibility χ_{max} was found near 12°K for all crystal axes, *a*, *b* and *c*. The experimental result was compared with the theoretical curve of magnetic susceptibility of antiferromagnetic linear chain spin systems given by Bonner and Fisher[1] who calculated an exact value of finite ring Heisenberg spin susceptibility. As is shown in Fig. 5, coincidence between theory and experiment is satisfactory if the intrachain exchange interaction J is taken to be
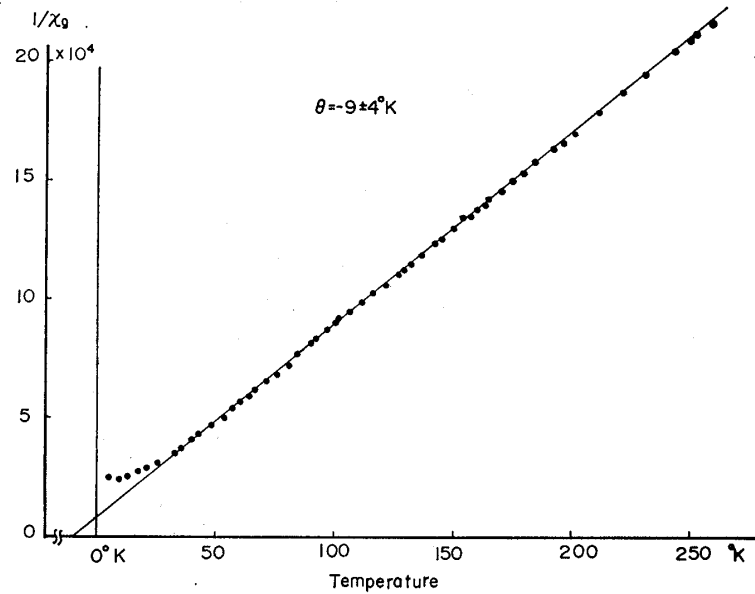
Fig. 3. Powdered paramagnetic susceptibility of copper benzoate. Temperature
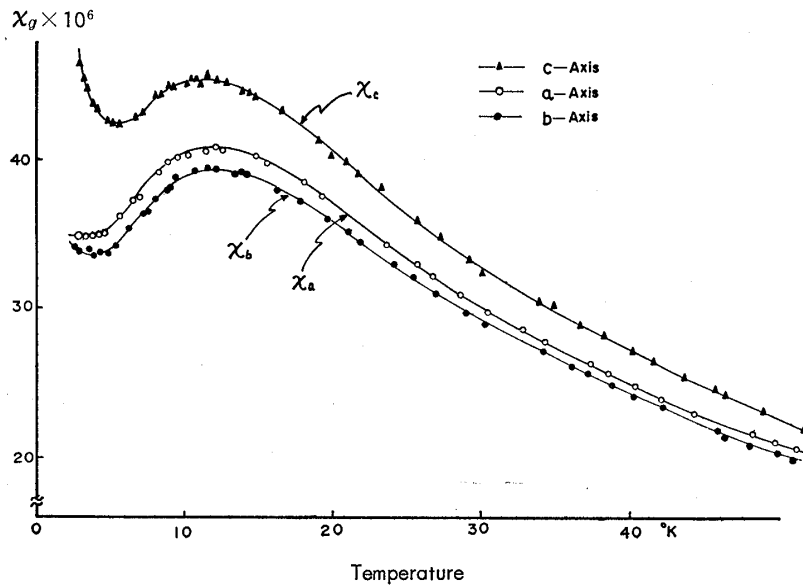independent part is removed.

Fig. 4. Magnetic susceptibilities along the crystallographic axes.

$$J/k = -8.6 \pm 0.5°K, \tag{1}$$

where J is defined as $-2JS_iS_j$ in the Hamiltonian. A deviation from the
Bonner-Fisher theory was observed for all directions below about 8°K. In
this temperature region the observed susceptibility is larger than the theoretical
value and shows an increasing tendency when temperature decreases. Similar
fact was observed in one dimensional antiferromagnet $KCuF_3$.[2] We did the
susceptibility measurement at various magnetic fields but no field dependence

was found. The magnetic torque measurement was done in *ab*-, *ac*- and *bc*-planes from 1.4 to 290°K and the conclusion is that there is no temperature dependence about the principal paramagnetic axes a', b and c'. This fact also shows that copper benzoate is paramagnetic even at 1.4°K.
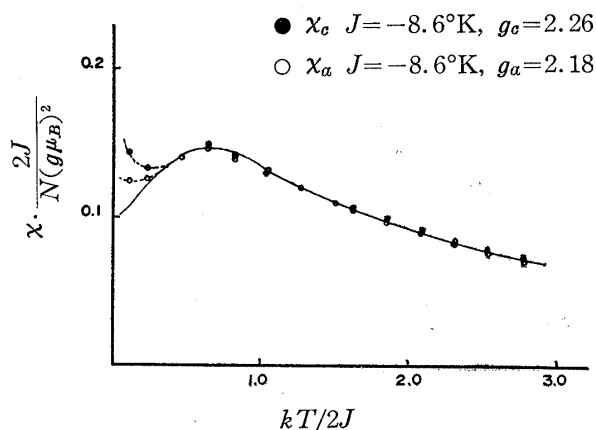
Fig. 5. Comparison of susceptibility data with Bonner-Fisher theory. Full line shows the theoretical curve extrapolated to an infinite chain. g-values were obtained by ESR study.

§5. Proton magnetic resonance and local magnetic field due to Cu^{2+} spins

The proton magnetic resonance study in a single crystal of copper benzoate was done by a standard nuclear resonance spectrometer. The steady method with a modulation frequency of 60 Hz was used and the *rf*-frequency was varied between 10 and 36 MHz. The temperature dependence of resonance signals was observed between 1.4 and 4.3°K. Above 4.2°K, a calibrated carbon resistor which was in contact with the *rf*-coil and the specimen, was used as a thermometer.

There are sixteen protons in a chemical formula of which ten protons are situated around two benzene rings and others belong to three water molecules. The resonance frequencies of the former ten protons come near the free proton frequency because the local magnetic field coming from copper spins is weak at the benzene sites. Accordingly, resonance lines due to these protons overlap to each other and the discrimination of these lines was practically impossible. On the other hand, protons belonging to the water molecules lie near Cu spins and show large shifts from the free proton position. Considering these facts, we discuss the magnetic resonance of protons coming from three water molecules. Figure 6 shows a projection of the crystal structure on the *ab*-plane. Of three water molecules, two H_2O nominated as $H_2O(1)$ contact directly to Cu ion but one molecule named $H_2O(2)$ locates between the tetrahedrons so that the local magnetic field on the proton position of $H_2O(1)$ is larger than that of $H_2O(2)$. So, we mainly analized the resonance signals coming from $H_2O(1)$ molecules. For convenience, these four protons are nominated as I, II, III and IV as are illustrated in Fig. 6. Paths of the hydrogen bond associating with these protons are also shown in the figure. Precise positions of these protons were determined using a general empirical rule of hydrogen
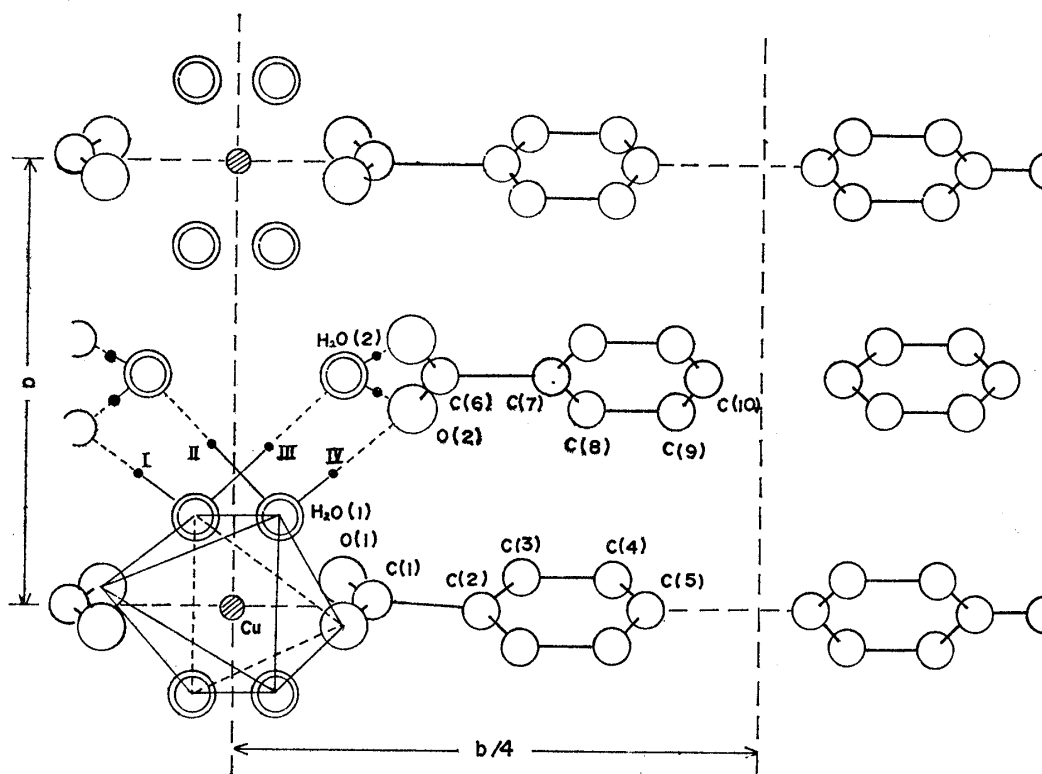
Fig. 6. Projection of crystal structure on the ab-plane. Black points show protons situated near Cu ions.

bonding.[8]

The angular dependence of proton resonance frequencies was investigated by rotating an external magnetic field in the ab, bc and ac-planes and an example is shown in Fig. 7. Figure 7(A) shows theoretical curves which were calculated by assuming dipolar fields coming from paramagnetic Cu spins and surrounding protons. The magnetization of Cu spins was estimated by the static susceptibility data. Since Bloembergen tried to calculate the angular dependence of proton resonance in hydrated compounds,[9] the method of calculation has been well established and can be used easily although the calculation is tedious. Figure 7(B) shows the corresponding experimental angular dependence in the ab-plane. Agreement between theory and experiment is satisfactory except small deviations. Thus, resonance lines corresponding to I, II, III and IV protons were easily identified. Similar results were obtained in the ac and bc-planes. Using these data, the magnetization of copper spins can be estimated as a function of temperature. An example due to this method is given in Fig. 8 where the magnetic susceptibility along the b-axis is evaluated. A broad maximum of the susceptibility was observed at $12.5\pm1°K$ showing a good agreement with the static susceptibility data. However, an interesting disagreement between the static and NMR susceptibilities appeared below about $8°K$ especially along the c-axis. As is shown in Fig. 9, the NMR susceptibility becomes very large as decreasing the temperature whereas the corresponding

susceptibility measured by the static method varies rather slowly with temperature. Origin of such a curious discrepancy is not known yet. The disagreement was not so large along the *b* and *a*-axes. As the data along the *a*-axis are very similar with those of the *b*-axis, they are not shown in Fig. 9.

Concerning with the low temperature anomaly of NMR susceptibility, the magnetic susceptibility in one dimensional antiferromagnet $KCuF_3$ should be remembered. Hirakawa and his collaborators[2] found that the static susceptibility in $KCuF_3$ shows a monotonic increasing as temperature decreases at low temperatures but the NMR susceptibility does not show such an increasing and follows exactly to the Bonner-Fisher curve.[3] So, there has been a doubt that the anomalous increase in the low temperature
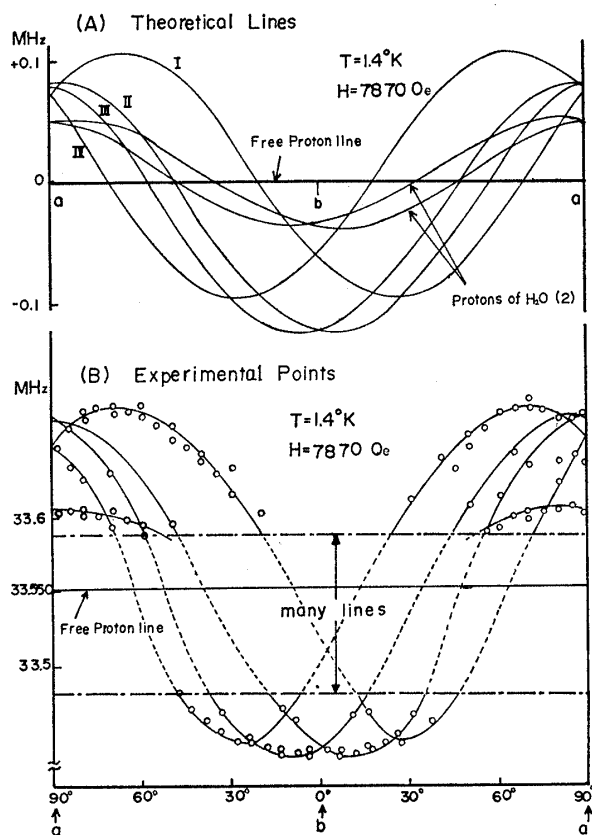

Fig. 7. Angular dependence of proton resonances in the *ab*-plane.

(A) shows theoretical curves with a relative scale from free protons.

(B) shows the experimental result except overlapped proton signals coming from benzene ring groups.
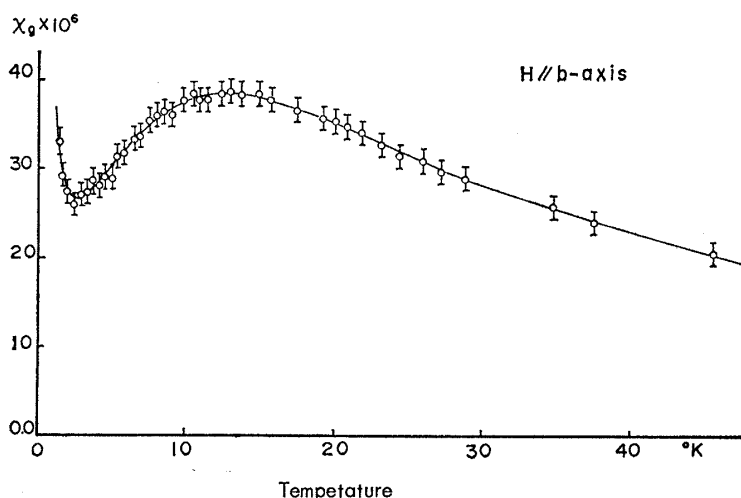

Fig. 8. Temperature dependence of Cu spin susceptibility estimated from proton resonance.

susceptibility might come from magnetic impurities. In copper benzoate, however, such an increase is rather large in NMR data. This fact suggests that there might be any other microscopic reasons for explaining the anomalous phenomenon.

§6. Electron spin resonance

Electron spin resonance was studied on a single crystal of copper benzoate using microwaves of 10 and 35 GHz regions. As was reported previously,[6] single paramagnetic resonance line was observed between 1.4 and 290°K with no resonance shift even near 1.4°K. The obtained angular dependences of the g-value are given in Fig. 10. The principal

Fig. 9. Comparison of the static and dynamic susceptibilities.

axes of the g-value in the ab and bc-planes coincide with the crystallographic axes but those in the ac-plane are apart from the a and c-axes and point along the a' and c'-axes as is expected in §2. The principal values of the resultant g-tensor were determined to be

$$\left.\begin{array}{l} g_{a'} = 2.08 \pm 0.02, \\ g_{b} = 2.06 \pm 0.02, \\ g_{c'} = 2.35 \pm 0.02. \end{array}\right\} \tag{2}$$

Noticing the fact that $g_{a'}$, g_b and $g_{c'}$ in Eq. (2) are amalgamated g-values of two inequivalent Cu spins I and II illustrated in Fig. 1, one can calculate the g-value of individual Cu spins and the results are given as

$$\left.\begin{array}{l} g_z = 2.36 \pm 0.02, \\ g_x = 2.07 \pm 0.02, \\ g_y = 2.05 \pm 0.02, \end{array}\right\} \tag{3}$$

where z means the tetragonal axis I or II and x and y show the principal axes perpendicular to it. Exactly speaking, the local magnetic symmetry is
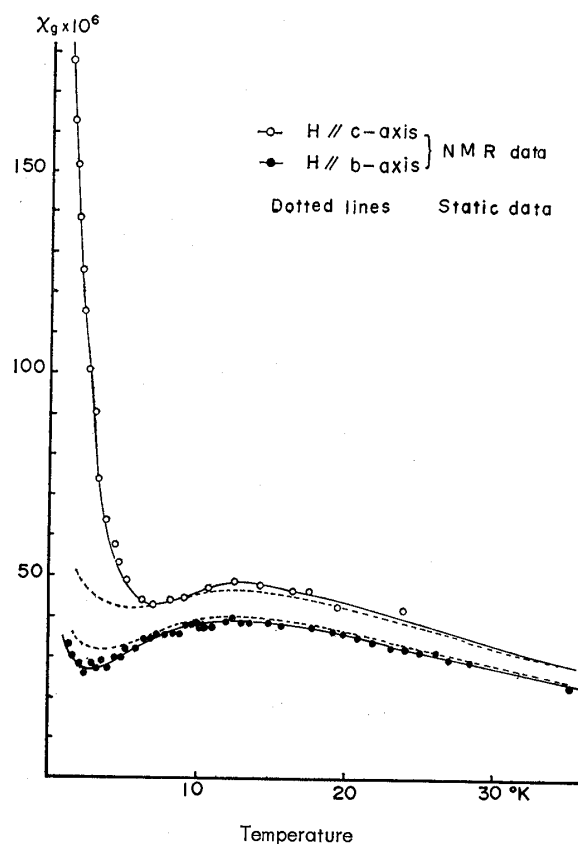
orthorhombic but one may regard the system as to be nearly tetragonal because $g_x - g_y$ is very small. Accordingly, we use hereafter the uniaxial g-value given by

$$\left. \begin{array}{l} g_{//} = 2.36, \\ g_{\perp} = 2.06. \end{array} \right\} \tag{4}$$

The resonance line width defined by the maximum slope width of 100 kHz field modulation signal showed interesting features. The width does not show frequency dependence at high temperatures but a strong angular dependence is seen in the ac-plane as is shown in Fig. 11. When temperature decreases down to liquid helium region, the width becomes narrow and at 4.2°K it reduces to about 1/4 compared with that at 290°K if microwave of 10 GHz region is used (Fig. 11(B)). At 35 GHz region, on the other hand, the width at 4.2°K also shows a narrowing tendency, but it is not so strong and the angular dependence is not so similar with the high temperature data. At 1.4°K, the angular dependence is very different. The result in the bc-plane is shown in Fig. 12. It is noticed that the center of symmetry in the ac-plane neither coincides to the a or c-axes nor to the magnetic axes a' or c'. The symmetry axes of the line width in the ac-plane point to new axes a'' and c'' which are apart about 15° from the a and c-axes, respectively. The reason will become clear in the next section.
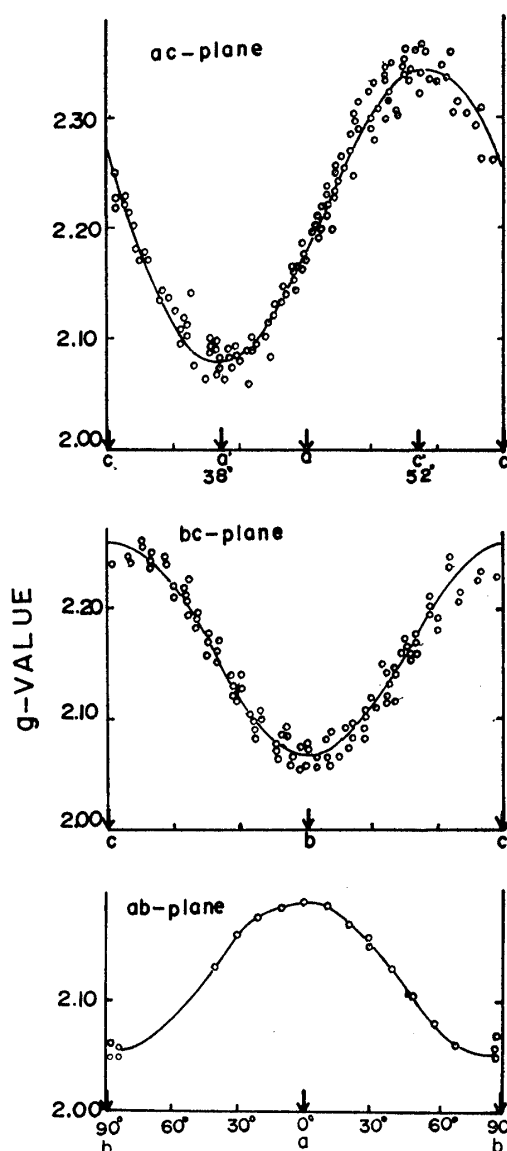

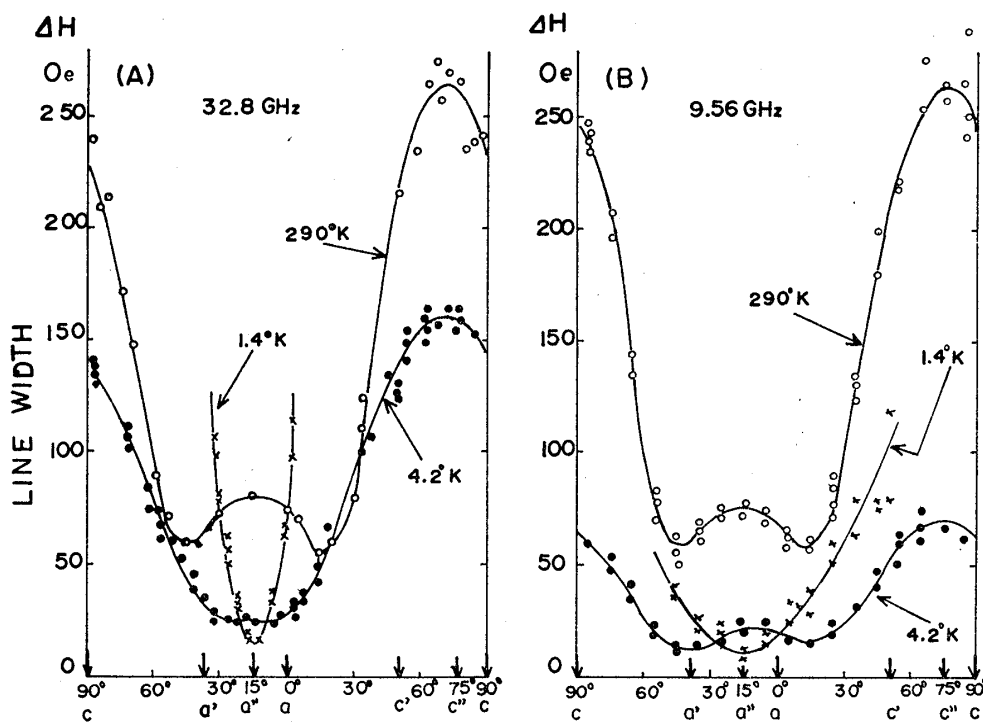Fig. 10. Angular dependences of g-value in copper benzoate.

Fig. 11. Angular and temperature dependences of the ESR line width in the ac-plane. Axes of the symmetry center are defined as a'' and c''.
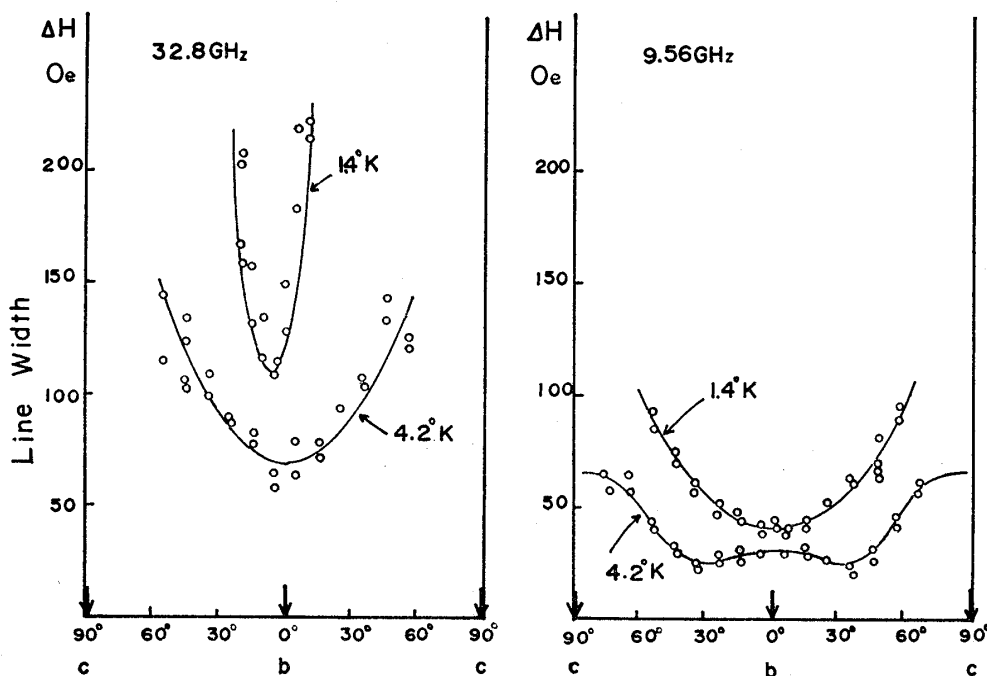
Fig. 12. Angular and temperature dependences of the ESR line width in the bc-plane.

§7. Effect of anisotropic exchange interactions on the ESR line width

It is well known that in paramagnetic crystals dipolar interaction broadens the ESR line width[10] and the exchange interaction between spins gives a narrowing effect.[11] These theoretical treatments were summarized by Kubo and Tomita[12] who developed a general theory of magnetic resonances based on the statistical theory of the spin system and the method to treat a para-magnetic resonance problem is now well established. To understand a few curious properties of the ESR line width especially in the *ac*-plane of the copper benzoate, it is emphasized that the usual treatment including the dipolar and isotropic exchange interactions is not enough even if one considered the line width at high temperatures only. For example, one cannot explain why the axes of symmetry center a'' and c'' differ by 15° rotation from the a and c-axes, respectively. Considering these facts, we tried to introduce the effect of anisotropic exchange interactions upon the line width. As is well known,[13] the magnitude of this interaction is of the order of $(\Delta g/g)^2 J$, with Δg an anisotropy of the g-tensor. Since J in a chain is large, this term cannot be neglected.

Now we investigate it according to the Kubo-Tomita theory using their notations. In addition to this effect, there may be a Dzyaloshinsky-Moriya term[14],[15] of which we also calculate but it may be small because an angle between two inequivalent tetragonal axes I and II as are shown in Fig. 1 is small. If this angle vanished, the Dzyaloshinsky-Moriya term would be elimi-nated. The Hamiltonian of the spin system can be written by

$$H = H_0 + H_e + H_d + H_{YM} + H_{DM},\tag{5}$$

where H_0 and H_e are the Zeeman and isotropic exchange terms, respectively and H_d represents the dipolar interaction. The last two terms show the an-isotropic exchange parts of which a symmetric anisotropic exchange is given by H_{YM} and an antisymmetric part is written as H_{DM}. Now we calculate the second moment of Eq. (5). First of all, the following relation is assumed:

$$H_e \gg H_0 \gg H_d, \; H_{YM}, \; H_{DM}.\tag{6}$$

A small relative anisotropy of the Zeeman energy due to inequivalence of spins is neglected. Then the perturbing Hamiltonian H' contributed to the second moment of the line width is given as

$$H' = H_d + H_{YM} + H_{DM}$$
$$= g^{*2}\mu_B^2 \sum_{k>j} \{ r_{jk}^{-3}(\boldsymbol{S}_j\,\boldsymbol{S}_k) - 3r_{jk}^{-5}(\boldsymbol{r}_{jk}\,\boldsymbol{S}_j)\,(\boldsymbol{r}_{jk}\,\boldsymbol{S}_k) \}$$
$$+ \sum_{k>j} \boldsymbol{S}_j\,\widetilde{A}_{jk}\,\boldsymbol{S}_k + \sum_{k>j} \boldsymbol{D}_{jk}\,[\boldsymbol{S}_j \times \boldsymbol{S}_k],\tag{7}$$

where g^* is the resultant g-value along the external magnetic field and μ_B shows the Bohr magneton. r_{jk} is the distance between spins S_j and S_k. The principal axes of the anisotropic exchange tensor $\widetilde{A}_{jk}$ coincide with those of the g-tensor as were experimentally verified in antiferromagnetic resonance.[16] Then $\widetilde{A}_{jk}$ is written as

$$\widetilde{A}_{jk} = \begin{pmatrix} A_{jk}^X & 0 & 0 \\ 0 & A_{jk}^Y & 0 \\ 0 & 0 & A_{jk}^Z \end{pmatrix}, \quad A_{jk}^X + A_{jk}^Y + A_{jk}^Z = 0, \tag{8}$$

being the X, Y and Z axes to be the a', b and c' axes, respectively. For simplicity, $\boldsymbol{D}_{jk}$ was assumed to have the same principal axes, X, Y and Z. According to the Kubo-Tomita theory, Eq. (7) is rewritten as follows:

$$\begin{aligned}
H' = &\sum_{k>j} \varPhi_{jk}^0 \{ S_j^z S_k^z - (1/4)(S_j^+ S_k^- + S_j^- S_k^+) \} \\
&+ \sum_{k>j} \varPhi_{jk}^{+1} \{ S_j^- S_k^z + S_j^z S_k^- \} + \sum_{k>j} \varPhi_{jk}^{-1} \{ S_j^+ S_k^z + S_j^z S_k^+ \} \\
&+ \sum_{k>j} \varPhi_{jk}^{+2} \{ S_j^- S_k^- \} + \sum_{k>j} \varPhi_{jk}^{-2} \{ S_j^+ S_k^+ \} \\
&+ \sum_{k>j} \varPsi_{jk}^0 \{ S_j^- S_k^+ - S_j^+ S_k^- \} \\
&+ \sum_{k>j} \varPsi_{jk}^{+1} \{ S_j^+ S_k^z - S_j^z S_k^+ \} + \sum_{k>j} \varPsi_{jk}^{-1} \{ S_j^z S_k^- - S_j^- S_k^z \},
\end{aligned} \tag{9}$$

where

$$\left.\begin{aligned}
\varPhi_{jk}^0 =& (A_{jk}^X \sin^2\gamma + A_{jk}^Z \cos^2\gamma) + g^{*2}\mu_B^2 r_{jk}^{-3}(1 - 3\cos^2\theta_{jk}), \\
\varPhi_{jk}^{\pm 1} =& (1/2)(A_{jk}^Z - A_{jk}^X)\sin\gamma\cos\gamma \\
&- (3/2)g^{*2}\mu_B^2 r_{jk}^{-3}\sin\theta_{jk}\cos\theta_{jk}\exp(\pm i\varphi_{jk}), \\
\varPhi_{jk}^{\pm 2} =& (1/4)(A_{jk}^X \cos^2\gamma + A_{jk}^Z \sin^2\gamma - A_{jk}^Y) \\
&- (3/4)g^{*2}\mu_B^2 r_{jk}^{-3}\sin^2\theta_{jk}\exp(\pm i\varphi_{jk}), \\
\varPsi_{jk}^0 =& (1/2i)(D_{jk}^Z \cos\gamma - D_{jk}^X \sin\gamma), \\
\varPsi_{jk}^{\pm 1} =& (1/2i)(D_{jk}^X \cos\gamma + D_{jk}^Z \sin\gamma + iD_{jk}^Y),
\end{aligned}\right\} \tag{10}$$

γ, θ_{jk} being angles between the Z-axis and external field, and the r_{jk} direction and external field, respectively. φ_{jk} is an azimuthal angle. In addition to dipolar terms which were discussed by Kubo and Tomita, two types of anisotropic exchange interactions are included in our treatment. Using techniques given by Kubo and Tomita, the following formulae of the second moment σ_T can be obtained:

$$\sigma_T^2 = \sigma_0^2 + \sigma_1^2 + \sigma_{-1}^2 + \sigma_2^2 + \sigma_{-2}^2, \tag{11}$$

where

$$\sigma_0^2 = \{3S(S+1)/4\hbar\}\sum_k \{\langle|\mathit{\Phi}_{jk}^0|^2\rangle + (16/9)\langle|\mathit{\Psi}_{jk}^0|^2\rangle\},$$

$$\sigma_1^2 = \{3S(S+1)/4\hbar\}\sum_k (16/9)\langle|\mathit{\Phi}_{jk}^1|^2\rangle,$$

$$\sigma_{-1}^2 = \{3S(S+1)/4\hbar\}\sum_k \{(8/3)\langle|\mathit{\Phi}_{jk}^{-1}|^2\rangle + (8/9)\langle|\mathit{\Psi}_{jk}^{-1}|^2\rangle\}, \qquad (12)$$

$$\sigma_2^2 = \{3S(S+1)/4\hbar\}\sum_k (16/9)\langle|\mathit{\Phi}_{jk}^2|^2\rangle,$$

$$\sigma_{-2}^2 = 0,$$

were obtained according to a standard procedure. Because of a strong exchange interaction in a chain, non secular terms $\sigma_{\pm 1}$ and $\sigma_{\pm 2}$ should be taken into account. As spins are placed on a rigid lattice, the time average operation $\langle\ \rangle$ in Eqs. (12) is not necessary.

Next, we discuss the observed angular dependence using these formulae. Firstly, we assume that the anisotropic exchange tensor $\widetilde{A}_{jk}$ is tetragonal. This assumption may be reasonable because the g-tensor is also nearly tetragonal.[16] Then one has a parameter A defined by

$$A = A_{jk}^Z = -2A_{jk}^X = -2A_{jk}^Y, \qquad (13)$$

for expressing a magnitude of the symmetric anisotropic exchange interaction. Suffices jk are not necessary because only one kind of exchange is considered along the chain. Secondly, D_{jk} terms are dropped out. We also calculated the effect of D_{jk} terms on the line width but it was found to be small so that it is omitted here, for simplicity. Thirdly, it is pointed out that the dipolar fields can practically be neglected except those coming from the nearest neighbor spins along the chain. To understand this, the following fact should be remembered: in a strongly exchange-narrowed line, the width is proportional to σ_T^2 in which the dipolar part coming from each spin is proportional to r_{jk}^{-6}. Since r_{jk} of the next neighbour interaction is $2r_0$, r_0 being the nearest neighbor spin spin distance, r_{jk}^{-6} equals $r_0^{-6}/64$. As the interchain distance is larger than r_0, the total contribution upon σ_T^2 except nearest neighbors remains to be about 5%. Accordingly, dipolar effect coming from distant spins can be neglected. Using Eqs. (10) and assumptions mentioned above, one obtains the following relations:

$$\langle|\mathit{\Phi}_{jk}^0|^2\rangle = (A/2)^2(3\cos^2\gamma - 1)^2 + B^2(3\cos^2\theta - 1)^2$$
$$- (AB/2)(3\cos^2\gamma - 1)(3\cos^2\theta - 1),$$

$$\langle|\mathit{\Phi}_{jk}^{\pm 1}|^2\rangle = (3A/4)^2 \sin^2\gamma \cos^2\gamma + (9/4)B^2 \sin^2\theta \cos^2\theta, \qquad (14)$$

$$\langle|\mathit{\Phi}_{jk}^{\pm 2}|^2\rangle = (3A/4)^2 \sin^4\gamma + (3B/4)^2 \sin^4\theta,$$

where a notation $B = g^*\mu_B r_0^{-3}$ is used. Then the resultant second moment can be calculated in the *ac*-plane as

$$\sigma_T^2 = \{(3/4)S(S+1)/\hbar\}\,[A^2\{\cos^2(\alpha-\theta)+1\}+4B^2(\cos^2\theta+1)$$

$$-AB\{3\cos^2(\alpha-\theta)-1\}(3\cos^2\theta-1)],\qquad\qquad(15)$$

where parameters α and θ are defined as are shown in Fig. 13. It is noticed that one can determine the sign of anisotropic exchange interaction A by investigating a role of the cross term with dipolar interaction (the third term in Eq. (15)). Since there is a strong exchange narrowing due to the intra-chain exchange interaction J, the second moment should be reduced by the exchange effect to obtain the width. This can be done by a standard method[12] and the result is shown in Fig. 14 as a theoretical curve (H_d+H_{YM}). Comparison with the experimental result at room temperature is satisfactory. A best coincidence was obtained when a ratio A/B was chosen to be

$$A/B=-0.84.\qquad\qquad(16)$$

This means that the effect of anisotropic exchange interaction is of the comparable order compared with the dipolar interaction. For comparison, the angular dependence of the line width due to the dipolar and isotropic exchange only $(H_d$ only) is shown in Fig. 14, which shows a fairly large disagreement with the experimental result. The magnitude of the anisotropic exchange constant A is written as

$$A\approx0.5(\Delta g/g)^2 J.\qquad\qquad(17)$$

This shows that the result agrees with the theoretical value estimated by Moriya and Yosida.[13]

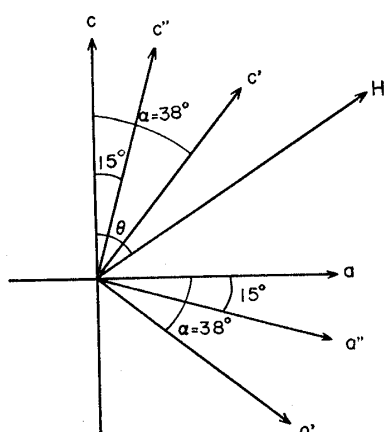A conclusion of this section can be expressed in the following way: The

Fig. 13. Angular relations of various axes in the ac-plane.
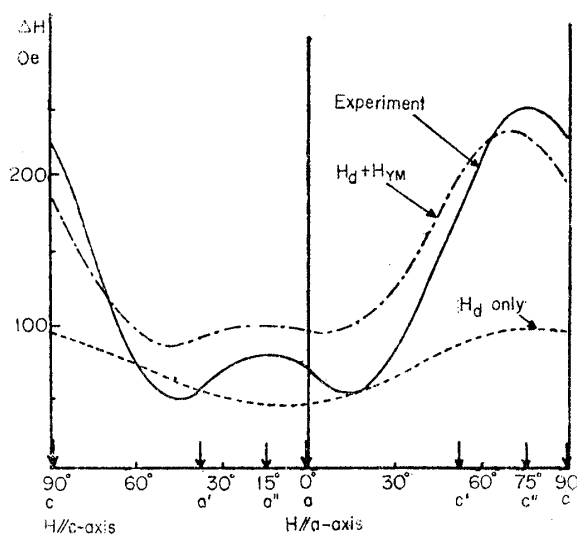
Fig. 14. Comparison of theoretical and experimental line widths at 290°K in the ac-plane.

paramagnetic resonance line width can be explained by considering the dipolar and anisotropic exchange interactions under a stong exchange narrowing condition but the success is limited only at high temperature regions. There are complex angular and frequency dependences when temperature decreases and these features are not yet explained.

Acknowledgement

The present authors are grateful to have a chance to submit the paper to a special issue for Professor Takeo Nagamiya.

References

1) J. C. Bonner and M. E. Fisher, Phys. Rev. **135A** (1964), 640.
2) S. Kadota, I. Yamada, Y. Yoneyama and K. Hirakawa, J. Phys. Soc. Japan **23** (1967), 751.
3) K. Hirakawa and S. Kadota, J. Phys. Soc. Japan **23** (1967), 756.
4) M. T. Hutchings, E. J. Samuelsen, G. Shirane and K. Hirakawa, Phys. Rev. **188** (1969), 919.
5) M. Ikebe and M. Date, to be published in J. Phys. Soc. Japan.
6) M. Date, M. Motokawa and H. Yamazaki, J. Phys. Soc. Japan **18** (1963), 911.
7) H. Koizumi, K. Osaki and T. Watanabé, J. Phys. Soc. Japan **18** (1963), 117.
8) S. Sato and S. Hoshino, J. Cryst. Soc. Japan **6** (1964), 85.
9) N. Bloembergen, Physica **16** (1950), 95.
10) J. H. Van Vleck, Phys. Rev. **74** (1948), 1168.
11) P. W. Anderson and P. R. Weiss, Rev. Mod. Phys. **25** (1953), 269.
12) R. Kubo and K. Tomita, J. Phys. Soc. Japan **9** (1954), 888.
13) J. H. Van Vleck, J. de Phys. et le Radium **12** (1951), 262.
    T. Moriya and K. Yosida, Prog. Theor. Phys. **9** (1953), 663.
14) I. Dzyaloshinsky, J. Phys. Chem. Solids **4** (1958), 241.
15) T. Moriya, Phys. Rev. **117** (1960), 635.
16) M. Date, J. Phys. Soc. Japan **16** (1961), 1337.